Nanoscale

Pressure-Induced Fluorescent Enhancement of FA_aPbBr_{2+a} Composite Perovskites

Journal:	*Nanoscale*
Manuscript ID	NR-COM-12-2018-009780.R1
Article Type:	Communication
Date Submitted by the Author:	25-Feb-2019

Complete List of Authors:	Nguyen, Lan Anh Thi ; Hanyang University, Department of Physics Minh, Duong Nguyen; Hanyang University, Department of Chemistry, Research Institute for Natural Sciences, Institute of Nano Science and Technology Yuan, Ye; b. Center for High Pressure Science and Technology Advanced Research Samanta, Sudeshna; Centre for High Pressure Science & Technology Advanced Research, Wang, Lin; Center for High Pressure Science & Technology Advanced Research , Zhang, Dongzhou; sadf Hirao, Naohisa; Japan Synchrotron Radiation Research Institute, Kim, Jaeyong; Hanyang University, Physics Kang, Youngjong; Hanyang University, Department of Chemistry, Research Institute for Natural Sciences, Institute of Nano Science and Technology

Nanoscale

COMMUNICATION

Pressure-Induced Fluorescent Enhancement of $FA_\alpha PbBr_{2+\alpha}$ Composite Perovskites

Received 00th January 20xx,
Accepted 00th January 20xx

DOI: 10.1039/x0xx00000x

www.rsc.org/

Lan Anh Thi Nguyen,[1,2] Duong Nguyen Minh,[3] Ye Yuan,[5] Sudeshna Samanta,[2,5] Lin Wang,[5] Dongzhou Zhang,[6] Naohisa Hirao,[7] Jaeyong Kim[1,2*], Youngjong Kang,[3,4*]

$FA_\alpha PbBr_{2+\alpha}$ composite perovskites consisting of 0D FA_4PbBr_6 and 3D $FAPbBr_3$ have been synthesized by a solid state reaction. Due to the endotaxy passivation of $FAPbBr_3$ by FA_4PbBr_6, $FAPbBr_3$ crystals were stably deformed without agglomeration from the cubic to the orthorhombic structure by compression, and which led to a significant PL enhancement.

Metal halide perovskites have received increasing attention due to their outstanding optical and electrical properties such as broad optical absorption, high photoluminescence quantum yield (PLQY) with broad color tunability, long charge diffusion length and high mobility.[1-7] The general formula of perovskite is $A_\alpha BX_{2+\alpha}$, where A, B, X are monovalent cation, divalent metal such as Pb^{2+}, and halogen anion such as Cl^-, Br^-, I^-, respectively. Inorganic Cs^+ ion or organic ammonium including methylammonium (MA, $CH_3NH_3^+$) or formamidinium (FA, $CH(NH_2)_2^+$) are often used for the cation A^+. In this case, α can be varied from 1 to 4. For the case of α = 1 (ABX_3), it forms typical three-dimensional (3D) structure, where the A^+ is surrounded by the network of corner sharing $[BX_6]^{4-}$ octahedra. Increasing α leads to the formation of the lower dimensional structures where the octahedral network is separated by the cation A^+, and ultimately zero-dimensional (0D) perovskites (A_4BX_6) are formed when α is increased to α = 4. The 0D perovskite structure consists of the isolated octahedra interspersed with the cations.[8,9] Among them, 3D perovskite nanoparticles have been extensively investigated as a promising material for light emitters. They offer wide bandgap tunability simply by changing their elemental composition. However their very low PLQY in solid state (typically less than 1%) which are compared to high PLQY in solution (~90%) hampers their application in LED.[10,11] While 0D perovskites have not been investigated as extensively as 3D perovskites, they are also of interest due to their strong quantum confinement and high stability. Since metal-halide-comprised octahedral are spatially confined, 0D perovskites show high exciton binding energy which is efficient for high PLQY. Unlike typical 3D perovskites, 0D perovskite nanocrystals exhibit comparable PLQY in both solution (65%) and solid state (56%).[9,12,13]

While the optical and electrical properties of perovskites have been tuned by changing the halide X^- or the size of nanoparticles,[11,14] they can also be altered by applying high pressure.[15] For example, the recent studies show that applying high pressure on 3D perovskites led to piezochromism, conductivity enhancement or/and phase transitions because of the bond length contraction and octahedral distortion in crystal structures.[15-19] However, photoluminescence properties of perovskites were significantly deteriorated under high pressure condition because of losing their quantum confinement by agglomeration.[19,20]

Herein, we report dramatic photoluminescence enhancement in the mixture of 0D and 3D formamidinium lead bromide perovskite (FA_4PbBr_6/$FAPbBr_3$) (hereafter named as $FA_\alpha PbBr_{2+\alpha}$ composite perovskite) under high pressure in the order of giga-pascal (GPa). The decay of perovskite photoluminescence in solid state or under pressure is known to be mainly due to the agglomeration of crystals. Hence some passivation techniques including polymer encapsulation and core-shell structures have been employed.[21,22] Recently, endotaxy passivation that crystals are covered with the same chemical elements but in different crystal structure was found to be very effective for stabilizing nanocrystals.[23,24] For example, Quan *et al*. found that the 3D $CsPbBr_3$ nanocrystals

[1]Department of Physics, Hanyang University, Seoul, 04763, Korea.
[2]HYU-HPSTAR-CIS High Pressure Research Center, Hanyang University, Seoul, 04763, Korea. Email: kimjy@hanyang.ac.kr
[3]Department of Chemistry, Hanyang University, Seoul, 04763, Korea.
[4]Research Institute for Natural Sciences and Institute of Nano Science and Technology, Hanyang University, Seoul, 04763, Korea. Email: youngjkang@hanyang.ac.kr
[5]Center for High Pressure Science & Technology Advanced Research, Shanghai 201203, China.
[6]Partnership for Extreme Crystallography, University of Hawaii at Manoa, Honolulu, HI 96822, USA
[7]Japan Synchrotron Radiation Research Institute, Hyogo 679-5198 Japan

Electronic Supplementary Information (ESI) available: [details of any supplementary information available should be included here]. See DOI: 10.1039/x0xx00000x

embedded in 0D Cs_4PbBr_6 matrix exhibited a remarkably high PLQY in solid state by the endotaxy passivation.[25] Similarly, 3D $FAPbBr_3$ can be stably passivated with 0D FA_4PbBr_6 and *vice versa*, when their lattices match each other. In this case, both 0D and 3D crystals can be stably deformed at high pressure condition without agglomeration, and which leads to the enhancement of PLQY due to the increased binding energy by structural distortion. To this end, $FA_\alpha PbBr_{2+\alpha}$ composite perovskites were prepared and characterized at the high pressure condition. Our experiments show that PL intensity of $FA_\alpha PbBr_{2+\alpha}$ composite perovskites was enhanced by 21 times under the high pressure comparing with that at ambient condition, and stable over multiple compression cycles.

$FA_\alpha PbBr_{2+\alpha}$ composite perovskites were prepared by employing a solid state reaction. Briefly, $PbBr_2$-DMSO complex was first prepared by following the procedures reported previously.[26] The completely dried $PbBr_2$-DMSO complex powder was then mixed with FABr powder in the glove box. Upon mixing, the white powder instantaneously turned to pale orange, and exhibited green fluorescence under UV (Figure 1a, S1). In contrast, the mixture of $PbBr_2$ and FABr barely showed PL in the same condition (Figure S1). The results of synchrotron-based powder X-ray diffraction (XRD) data confirmed that the sample contained two different crystal structures, FA_4PbBr_6 ($R\bar{3}c$, $a = b = 13.07$ Å, $c = 18.45$ Å) and $FAPbBr_3$ perovskites ($Pm\bar{3}m$, $a = b = c = 5.99$ Å) (Figure 1b). The refinement results of general structure refinement system (GSAS) to the measured XRD data are presented in Figure S2. Based on the matching with the main diffracted peak positions and normalized amount of peak intensity, it was expected that FA_4PbBr_6 perovskite was dominant over $FAPbBr_3$ one. Due to the relatively large excess amount of FA_4PbBr_6, $FAPbBr_3$ was expected to be embedded within FA_4PbBr_6 matrix. In this case, endotaxy passivation of $FAPbBr_3$ by FA_4PbBr_6 was expected because of their close lattice matching (Table S3, Figure S3). Since the resulting $FA_\alpha PbBr_{2+\alpha}$ composite perovskites were easily hydrolyzed at ambient condition, all experiments were performed under inert

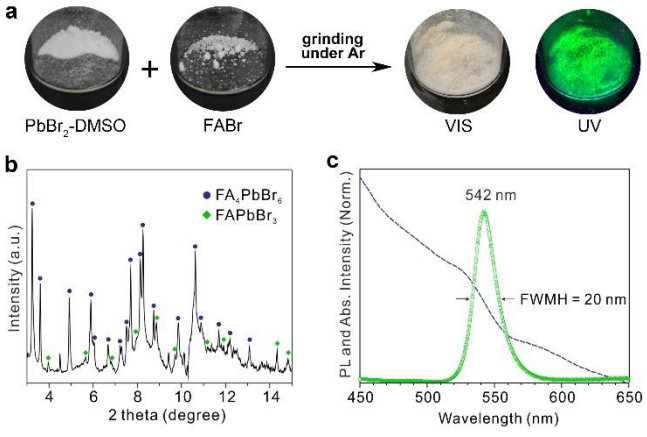

Figure 1. a) Preparation of $FA_\alpha PbBr_{2+\alpha}$ composite perovskite by a solid state mixing of $PbBr_2$-DMSO and FABr powders. Upon mixing, the mixtures exhibited strong green fluorescent under UV illumination. b) XRD pattern of $FA_\alpha PbBr_{2+\alpha}$ composite perovskite which shows that the resulting compound was the mixture of 0D FA_4PbBr_6 and 3D $FAPbBr_3$. The expected peak positions for 0D and 3D structures from the GSAS calculation are marked on the pattern. c) PL and UV-Vis absorbance spectra of the $FA_\alpha PbBr_{2+\alpha}$ composite perovskite.

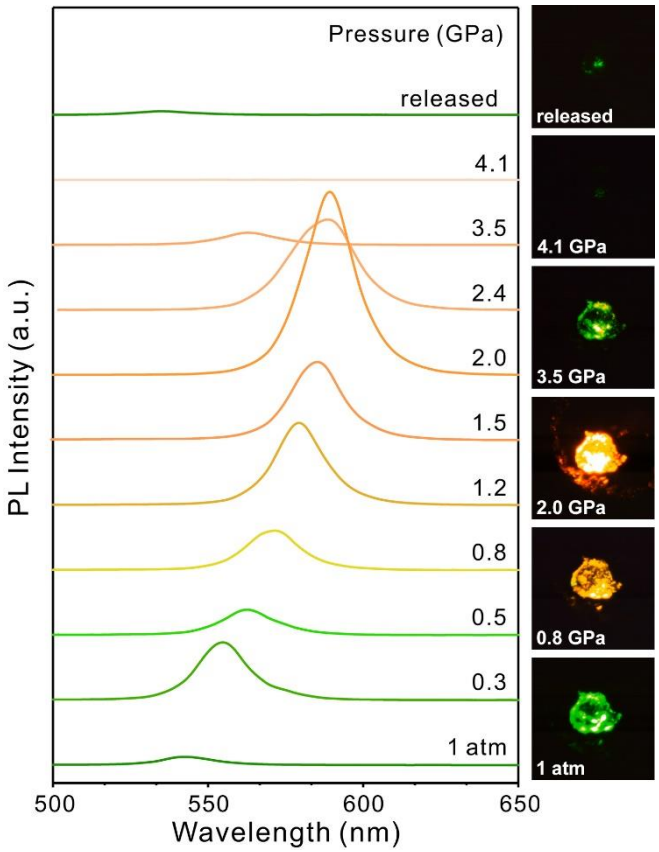

Figure 2. Pressure-induced PL changes of $FA_\alpha PbBr_{2+\alpha}$ composite perovskite. Spectra and fluorescent optical image of a $FA_\alpha PbBr_{2+\alpha}$ composite perovskite were taken *in situ* while increasing the pressure from 1 atm to 4.1 GPa.

condition. The PL spectrum of $FA_\alpha PbBr_{2+\alpha}$ composite perovskite was almost same as that of pure $FAPbBr_3$ perovskite nanoparticles deposited on a Si substrate.[26,27] UV-Vis data also supported the formation of $FA_\alpha PbBr_{2+\alpha}$ composite perovskite. The absorbance spectra of the mixture showed the existence of strong and narrow absorbance peak at 325 nm which was originated from FA_4PbBr_6 perovskite (Figure 3a),[28] and a gentle slope at 540 nm corresponding to the absorption peak of $FAPbBr_3$ (Figure 1c, 3b).[26] All these data support well the formation of $FA_\alpha PbBr_{2+\alpha}$ composite perovskite by the simple solid-state reaction of $PbBr_2$-DMSO and FABr powders.

The high pressure experiments were carried out by using a symmetric diamond anvil cell (DAC). $FA_\alpha PbBr_{2+\alpha}$ composite perovskites were pressurized by silicon oil as a pressure medium in a DAC. Ruby was used as a pressure marker. PL and fluorescent optical microscope images of $FA_\alpha PbBr_{2+\alpha}$ composite perovskite were taken *in situ* while changing pressure (Figure 2). Under ambient condition, $FA_\alpha PbBr_{2+\alpha}$ composite perovskite showed a green fluorescent emission at $\lambda_{peak} = 542$ nm. The PL spectrum corresponded to that of pure $FAPbBr_3$,[26] which suggests that PL of $FA_\alpha PbBr_{2+\alpha}$ composite perovskite was mainly due to $FAPbBr_3$. The green emission was gradually turned to orange with increasing the pressure until 2.0 GPa, and then turned back to green as the pressure increased further (Figure 2). When the pressure increased further above 4.1 GPa, the fluorescent almost disappeared. After releasing the pressure, however, the sample recovered the green fluorescence. Such

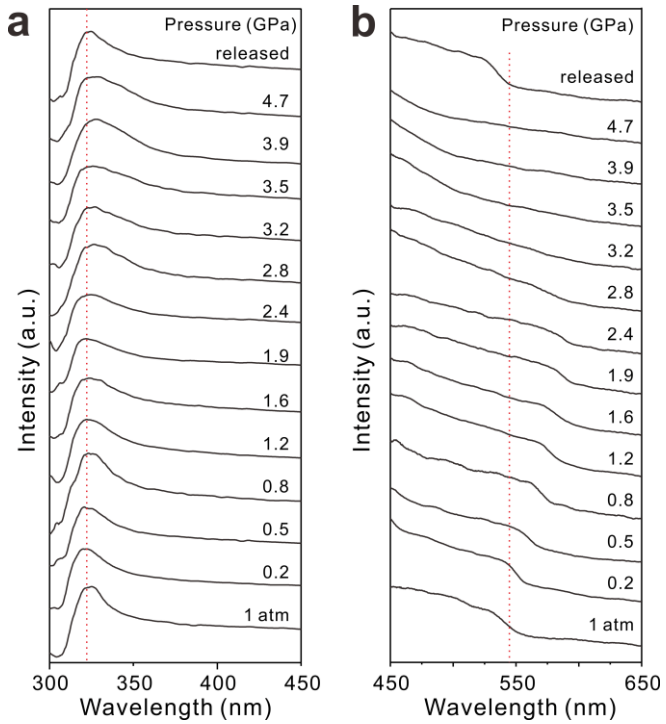

Figure 3. UV-Vis absorbance spectra of $FA_\alpha PbBr_{2+\alpha}$ composite perovskite as a function of the applied pressure. a) The peak at 325 nm originated from FA_4PbBr_6 was insensitive to the change of the pressure. b) The band at 540 nm originated from $FAPbBr_3$ was persistently shifted to the longer wavelength as the pressure increased to 2.4 GPa, and then the feature disappeared above 2.8 GPa. After released the pressure, the band was recovered, but shifted slightly to the shorter wavelength (535 nm).

changes of photoemission color were almost the same as other previous reports on the pressure-induced PL changes of pure $FAPbBr_3$ perovskite.[16] In the aspect of PL intensity, however, $FA_\alpha PbBr_{2+\alpha}$ composite perovskite represented different responses from other pure 3D perovskites under high-pressure.[19,20] While PL of pure 3D perovskites mostly decreased with the pressure, PL of $FA_\alpha PbBr_{2+\alpha}$ composite perovskite gradually increased showing the maximum intensity at 2.0 GPa (Figure 2). The PL enhancement factor (f) was f = 21 at 2.0 GPa, where f was defined as the ratio of the PL intensity at a certain pressure to the intensity at 1 atm. Such dramatic enhancement of PL suggests that the agglomeration of $FAPbBr_3$ perovskite was effectively restricted during the compression. As increasing the pressure, the PL peak consistently shifted to the longer wavelength (λ_{peak} = 542 ~ 589 nm) until the pressure reached to 2.0 GPa, followed by a blue-shift with the decrease of the intensity at the higher pressure (> 2.0 GPa). The PL spectra persistently maintained the narrow bandwidth, full width at half maximum (FWHM) = 20 nm during the PL shift. The detail information of bandwidth and peak position of PL spectra as varying pressure is presented in Table S1. Above 3.5 GPa, PL almost disappeared presumably due to the pressure-induced amorphorization of $FAPbBr_3$.[16] It is noteworthy to mention that the pressure-induced PL enhancement was repeatable. After the first cycle of the compression, the $FA_\alpha PbBr_{2+\alpha}$ composite perovskite showed the same PL response during the subsequent second cycle. This result suggests that $FAPbBr_3$ perovskites were stably passivated without agglomeration by compression.

The pressure-induced phase transition of $FA_\alpha PbBr_{2+\alpha}$ composite perovskite was also apparent in UV-Vis spectra. As shown in Figure 3a, the absorbance peak at 325 nm corresponding to FA_4PbBr_6 was almost insensitive to the change of pressure up to 4.7 GPa. However, $FAPbBr_3$ peak at 540 nm gradually shifted to the longer wavelength until 2.4 GPa (λ_{peak} = 588 nm), and subsequently disappeared at higher pressure (> 3.2 GPa) (Figure 3b). After releasing the pressure, the band of $FAPbBr_3$ was recovered, but was slightly shifted to the shorter wavelength (535 nm). The values of optical bandgaps were estimated from UV-Vis spectra (Figure S4).[29] Due to the redshift of the absorbance edge during the compression, the bandgap was decreased.[16] The increase of band gap after releasing the pressure indicates the formation of small or thin layered $FAPbBr_3$.[30-32]

To correlate the optical properties with the structure, *in situ* high pressure XRD patterns of $FA_\alpha PbBr_{2+\alpha}$ composite perovskite were analyzed as a function of pressure (Figure 4). As increasing pressure, the main diffraction peaks of both $FAPbBr_3$ and

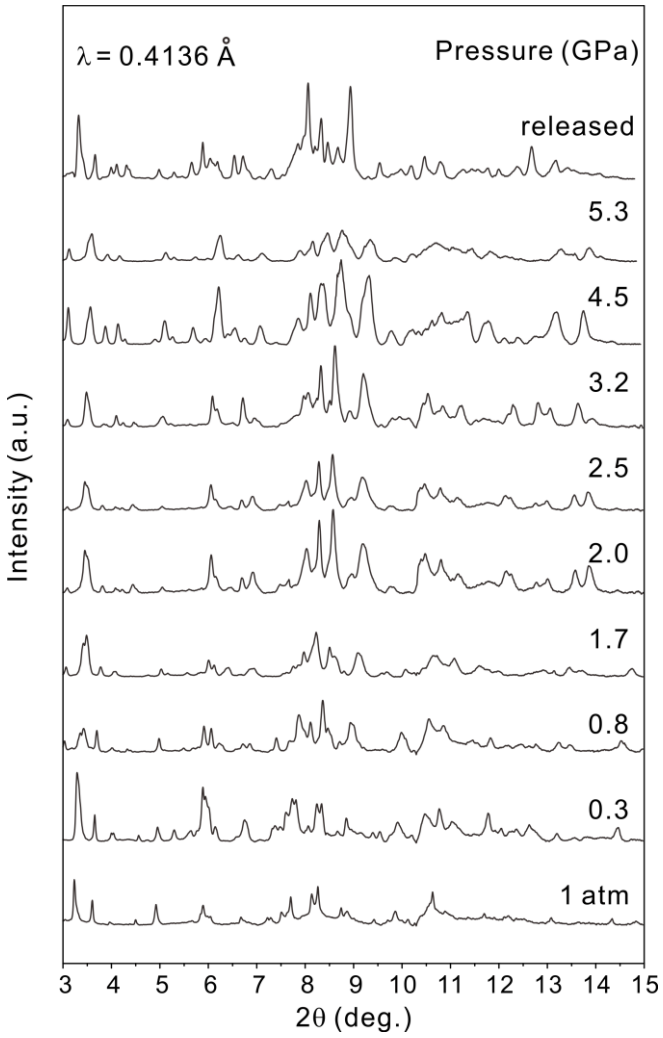

Figure 4. XRD patterns of $FA_\alpha PbBr_{2+\alpha}$ composite perovskite with varying the pressure from 1 atm to 5.3 GPa.

FA_4PbBr_6 shifted to the higher angle. Results of GSAS refinement revealed that the crystal structure of FA_4PbBr_6 ($R\bar{3}c$, $a = b = 13.07$ Å, $c = 18.45$ Å) was retained but slightly distorted at 5.3 GPa. On the contrary, the crystal structure of $FAPbBr_3$ exhibited strong pressure-dependent transitions: $Pm\bar{3}m$ ($a = b = c = 5.99$ Å) at 1 atm, $Im\bar{3}$ ($a = b = c = 11.12$ Å) at 0.8 GPa, and *Pnma* ($a = 8.18$ Å, $b = 11.44$ Å, $c = 8.49$ Å) at 2.0 GPa. These analyses indicate that the PL change by compression was mainly because of the pressure-induced transition of a cubic to an orthorhombic $FAPbBr_3$, which was induced by shrinking and tilting of $[PbBr_6]^{4-}$ octahedral.[16] In this case, FA_4PbBr_6 did not directly contribute to the PL enhancement, but stabilized $FAPbBr_3$ by endotaxy passivation. After 3.0 GPa, the shape of the broaden and weaken peaks suggests the gradual amorphorization process, which was responsible for the disappearing of PL. The original $Pm\bar{3}m$ crystal structure of $FAPbBr_3$ was recovered after releasing the pressure to 1 atm (detail shown in Figure S2). It was shown that the lattice mismatch was maintained low during the compression (Table S3). After the pressure release, two crystals ($FAPbBr_3$ and FA_4PbBr_6) were conformed within a lattice mismatching of less than 1 %.

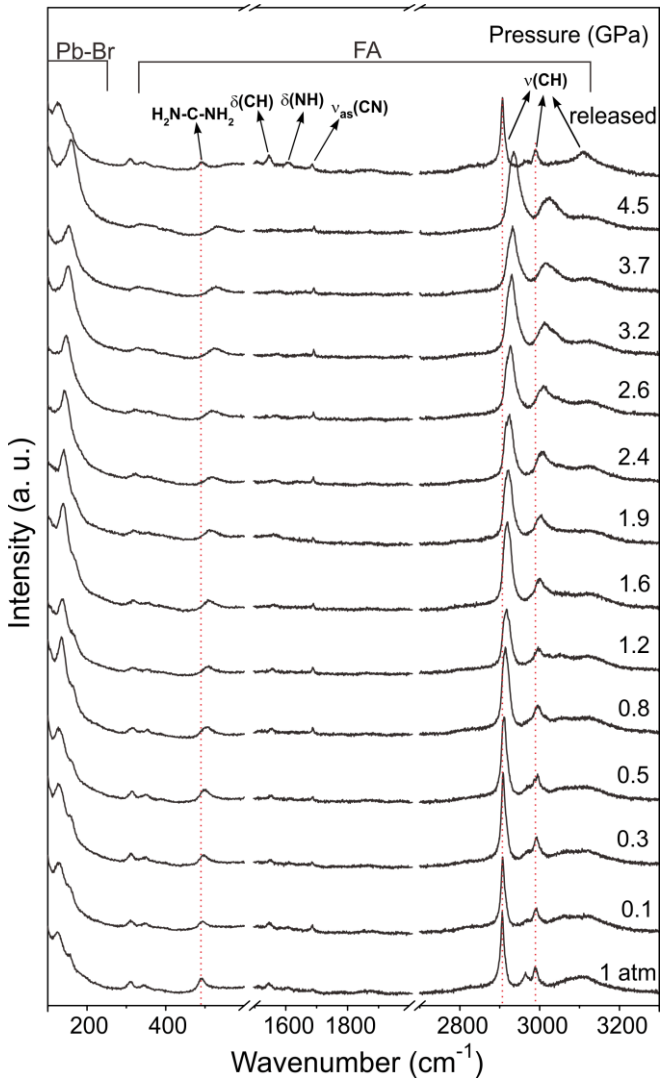

Figure 5. Plots of *in situ* high pressure Raman spectra of $FA_\alpha PbBr_{2+\alpha}$ composite perovskite.

The changes in Pb-Br networks had a central impact on the phase transition of $FA_\alpha PbBr_{2+\alpha}$ composite perovskite. High-pressure *in situ* Raman experiments were performed to investigate the dynamics of the organic FA^+ cation and the inorganic $[PbBr_6]^{4-}$ octahedral during the compression. As shown in Figure 5, the characteristic Raman peaks of FA and Pb-Br bonds successively shifted to the higher wavenumber, which presents the decreased bond length of Pb-Br and FA by compression. Broadening of vibrational peaks is due to an amorphorization which was resulted from the large distortion of FA cations under high pressure.[33, 34]

All data shown above revealed that PL enhancement of $FA_\alpha PbBr_{2+\alpha}$ composite perovskite during the compression was mainly originated from 3D $FAPbBr_3$ passivated by 0D FA_4PbBr_6. The original cubic structure of $FAPbBr_3$ crystal was distorted to the orthorhombic structure as increasing pressure to 2.0 GPa, and which leads to the enhancement of PL with the factor of $f = 21$. While $FAPbBr_3$ exhibited a strong PL enhancement by phase transitions, FA_4PbBr_6 did not directly contribute to the PL enhancement, but stabilized $FAPbBr_3$ by endotaxy passivation. XRD analysis showed that the lattice mismatch was kept low (<1%) during the phase transition of $FAPbBr_3$ by compression. Because of the endotaxy passivation, $FAPbBr_3$ exhibited the same pressure-induced PL changes for the subsequent multiple compression cycles (Figure S5).

Conclusions

In summary, 0D-3D $FA_\alpha PbBr_{2+\alpha}$ composite perovskites have been synthesized by solid state reaction, and their optical properties under high pressure have been investigated. The PL of $FA_\alpha PbBr_{2+\alpha}$ composite perovskites was tuned from 542 nm to 589 nm with the narrow FWHM around 20 nm by compression. Due to the endotaxy passivation of $FAPbBr_3$ by FA_4PbBr_6, $FAPbBr_3$ crystal structure was reversibly deformed by compression from an original cubic to an orthorhombic structure without agglomeration, and which led to significant enhancement of PL intensity with a factor of $f = 21$. In this case, FA_4PbBr_6 stabilized $FAPbBr_3$ rather than directly contributing PL enhancement. Our findings provide clues for stable and optimized optoelectronic devices based on metal halide perovskites.

Conflicts of interest

In accordance with our policy on Conflicts of interest please ensure that a conflicts of interest statement is included in your manuscript here. Please note that this statement is required for all submitted manuscripts. If no conflicts exist, please state that "There are no conflicts to declare".

Acknowledgements

This research was supported by Basic Science Research Program through the National Research Foundation of Korea (NRF) funded by the Ministry of Education, Science and Technology (NRF-2016K1A4A3914691, 2012R1A6A1029029 and 2017K2A9A1A06037779). High pressure experiments were performed at GeoSoilEnviroCARS (Sector 13), Partnership for Extreme Crystallography program (PX^2), Advanced Photon Source (APS), and Argonne National Laboratory. GeoSoilEnviroCARS is supported by the National Science Foundation-Earth Sciences (EAR-1634415) and Department of Energy-Geosciences (DE-FG02-94ER14466). PX^2 program is supported by COMPRES under NSF Cooperative Agreement EAR-1661511. Use of the Advanced Photon Source was supported by the US Department of Energy, Office of Science, Office of Basic Energy Sciences, under Contract No. DE-C02-6CH11357.

Notes and references

1. A. Kojima, K. Teshima, Y. Shirai and T. Miyasaka, *J. Am. Chem. Soc.*, 2009, **131**, 6050-6051.
2. M. M. Lee, J. Teuscher, T. Miyasaka, T. N. Murakami and H. J. Snaith, *Science*, 2012, 1228604.
3. A. Kojima, M. Ikegami, K. Teshima and T. Miyasaka, *Chem. Lett.*, 2012, **41**, 397-399.
4. H.-S. Kim, C.-R. Lee, J.-H. Im, K.-B. Lee, T. Moehl, A. Marchioro, S.-J. Moon, R. Humphry-Baker, J.-H. Yum and J. E. Moser, *Sci. Rep.*, 2012, **2**, 591.
5. J. Burschka, N. Pellet, S.-J. Moon, R. Humphry-Baker, P. Gao, M. K. Nazeeruddin and M. Grätzel, *Nature*, 2013, **499**, 316.
6. H. J. Snaith, *J. Phys. Chem. Lett.*, 2013, **4**, 3623-3630.
7. S. Ananthakumar, J. R. Kumar and S. M. Babu, *J. Photonics Energy*, 2016, **6**, 042001.
8. B. Saparov and D. B. Mitzi, *Chem. Rev.*, 2016, **116**, 4558-4596.
9. Y. Zhang, M. I. Saidaminov, I. Dursun, H. Yang, B. Murali, E. Alarousu, E. Yengel, B. A. Alshankiti, O. M. Bakr and O. F. Mohammed, *J. Phys. Chem. Lett.*, 2017, **8**, 961-965.
10. Y. Kim, E. Yassitepe, O. Voznyy, R. Comin, G. Walters, X. Gong, P. Kanjanaboos, A. F. Nogueira and E. H. Sargent, *ACS Appl. Mater. Interfaces*, 2015, **7**, 25007-25013.
11. L. Protesescu, S. Yakunin, M. I. Bodnarchuk, F. Krieg, R. Caputo, C. H. Hendon, R. X. Yang, A. Walsh and M. V. Kovalenko, *Nano Lett.*, 2015, **15**, 3692-3696.
12. M. I. Saidaminov, J. Almutlaq, S. Sarmah, I. Dursun, A. A. Zhumekenov, R. Begum, J. Pan, N. Cho, O. F. Mohammed and O. M. Bakr, *ACS Energy Lett.*, 2016, **1**, 840-845.
13. F. Zhang, H. Zhong, C. Chen, X.-g. Wu, X. Hu, H. Huang, J. Han, B. Zou and Y. Dong, *ACS Nano*, 2015, **9**, 4533-4542.
14. J. Xu, S. Xu, Z. Qi, C. Wang, C. Lu and Y. Cui, *Nanoscale*, 2018, **10**, 10383-10388.
15. A. Jaffe, Y. Lin and H. I. Karunadasa, *ACS Energy Lett.*, 2017, **2**, 1549-1555.
16. L. Wang, K. Wang and B. Zou, *J. Phys. Chem. Lett.*, 2016, **7**, 2556-2562.
17. A. Jaffe, Y. Lin, W. L. Mao and H. I. Karunadasa, *J. Am. Chem. Soc.*, 2017, **139**, 4330-4333.
18. P. Wang, J. Guan, D. T. Galeschuk, Y. Yao, C. F. He, S. Jiang, S. Zhang, Y. Liu, M. Jin and C. Jin, *J. Phys. Chem. Lett.*, 2017, **8**, 2119-2125.
19. G. Xiao, Y. Cao, G. Qi, L. Wang, C. Liu, Z. Ma, X. Yang, Y. Sui, W. Zheng and B. Zou, *J. Am. Chem. Soc.*, 2017, **139**, 10087-10094.
20. P. Postorino and L. Malavasi, *J. Phys. Chem. Lett.*, 2017, **8**, 2613-2622.
21. E. Ryu, S. Kim, E. Jang, S. Jun, H. Jang, B. Kim and S.-W. Kim, *Chem. Mater.*, 2009, **21**, 573-575.
22. S. A. Ivanov, A. Piryatinski, J. Nanda, S. Tretiak, K. R. Zavadil, W. O. Wallace, D. Werder and V. I. Klimov, *J. Am. Chem. Soc.*, 2007, **129**, 11708-11719.
23. L.-D. Zhao, J. He, S. Hao, C.-I. Wu, T. P. Hogan, C. Wolverton, V. P. Dravid and M. G. Kanatzidis, *J. Am. Chem. Soc.*, 2012, **134**, 16327-16336.
24. Z. Ning, X. Gong, R. Comin, G. Walters, F. Fan, O. Voznyy, E. Yassitepe, A. Buin, S. Hoogland and E. H. Sargent, *Nature*, 2015, **523**, 324.
25. L. N. Quan, R. Quintero-Bermudez, O. Voznyy, G. Walters, A. Jain, J. Z. Fan, X. Zheng, Z. Yang and E. H. Sargent, *Adv. Mater.*, 2017, **29,** 1605945.
26. D. N. Minh, J. Kim, J. Hyon, J. H. Sim, H. H. Sowlih, C. Seo, J. Nam, S. Eom, S. Suk and S. Lee, *Chem. Mater.*, 2017, **29**, 5713-5719.
27. L. Protesescu, S. Yakunin, M. I. Bodnarchuk, F. Bertolotti, N. Masciocchi, A. Guagliardi and M. V. Kovalenko, *J. Am. Chem. Soc.*, 2016, **138**, 14202-14205.
28. L. Wu, H. Hu, Y. Xu, S. Jiang, M. Chen, Q. Zhong, D. Yang, Q. Liu, Y. Zhao and B. Sun, *Nano Lett.*, 2017, **17**, 5799-5804.
29. J. Tauc, R. Grigorovici and A. Vancu, *Phys. Status Solidi B*, 1966, **15**, 627-637.
30. A. M. Smith and S. Nie, *Acc. Chem. Res.*, 2009, **43**, 190-200.
31. D. Li, G. Wang, H.-C. Cheng, C.-Y. Chen, H. Wu, Y. Liu, Y. Huang and X. Duan, *Nat. Commun.*, 2016, **7**, 11330.
32. T. Yin, Y. Fang, W. K. Chong, K. T. Ming, S. Jiang, X. Li, J. L. Kuo, J. Fang, T. C. Sum and T. J. White, *Adv. Mater.*, 2018, **30**.
33. L. Wang, K. Wang, G. Xiao, Q. Zeng and B. Zou, *J. Phys. Chem. Lett.*, 2016, **7**, 5273-5279.
34. R. G. Niemann, A. G. Kontos, D. Palles, E. I. Kamitsos, A. Kaltzoglou, F. Brivio, P. Falaras and P. J. Cameron, *J. Phys. Chem. C*, 2016, **120**, 2509-2519.